Telluride Te_2I: Electronic properties of one-dimensional atomic chains structure

Biaohua Wei[1] and Xu Han

[1]College of Electronic and Optical Engineering, Nanjing University of Posts and Telecommunications, Nanjing, Jiangsu, 210023, China

Abstract: Semiconductor tellurium is an excellent performance material, tellurium and its compounds have been extensive researched in the low-dimensional field. Inspired by the synthesis of a one-dimensional tellurium atomic chains, we predict a new one-dimensional Te_2I single-atomic chain structure based on first-principles. Using first-principles calculations, Te_2I single-atomic chain has an exfoliated energy of 137.95 meV, suggesting that the exfoliation of atomic chains materials from the bulk phase could be feasible. The single-atomic chain structure is an indirect band gap semiconductor with a band gap of 1.51 eV. In addition, its dynamic and thermodynamic properties indicate that the structure is stable at room temperature. Remarkably, it exhibits good electronic conductivity and a large difference in electron and hole mobilities, indicating that it is favorable for the migration and separation of photogenerated carriers. The absorption spectrum of one-dimensional Te_2I single-atomic chain exhibits a strong light-harvesting ability in the ultraviolet region, suggesting its potential application in optoelectronic devices.

1 Introduction

One-dimensional (1D) semiconductor materials have been widely studied due to their unique properties in photonics, electronics, and optoelectronics. [1-2] 1D materials can provide opportunities for the design of higher capacity and stable electrode materials, including the design of transistors with the smallest possible dimensions and chemical sensors that are extremely sensitive to the environment, and the interpretation of unique electronic phenomena caused by the similarity of fiber and ballistic electrons in 1D wires.[3-7]

Among various semiconductor materials, tellurium(Te) is a valuable p-type narrow band gap material, and it has shown good application potential in photoelectric and catalysis. [8-10] Te element can be combined with many elements to synthesize excellent 1D tellurides, such as $CoTe_2$, ZnTe, and CdTe.[11-13] 1D Te crystal has a unique DNA-like structure, in which atoms are strongly bonded to helical chains. Therefore, the Te system is formed by helical chains stack through weak van der Waals (vdW) interactions.[14] This 1D vdW crystal structure allows Te crystal to be isolated to few atomic chains or single-chain limit while maintaining the integrity of crystals.[15] The isolated 1D Te atomic chains crystal has good structural properties and has shown potential for application in the field of optoelectronics.[16] The crystallization method of Te crystal has inspired us to study the 1D atomic structure of telluride. Existing studies have shown that Te can form stable tellurium sub-halides crystallize Te_2I and Te_3Cl_2 with halogen elements. Due to all tellurium sub-halides crystallize are coordinated by halogen elements according to the arrangement of the Te element's threefold screw axis, they exhibit similar structural properties to Te crystals.[17]

Interestingly, there are also interchain vdW interaction forces in the bulk Te_2I system. [18] Since the atomic Te chain was successfully separated from the bulk Te by mechanical exfoliation, it should be feasible to prepare a 1D Te_2I atomic chains from the bulk Te_2I system in the experiment.[16] Therefore, we theoretically predict an indirect band gap 1D Te_2I single-atomic chain crystal with a band gap of 1.51 eV based on first principles. The molecular dynamics and thermodynamics of the 1D single-atomic chain structure are stable, and have strong covalent bonding capabilities. It has large carrier mobility and obvious absorption spectrum, suggesting that it is expected to be used in microelectronics and optoelectronic devices.

2 Computational details

Structural optimization and properties calculations in this study are based on density functional theory(DFT),as implemented in the Cambridge Sequential Total Energy Package (CASTEP) module.[19] The generalized gradient approximation is used in the Perdew Burke Ernzerhof (PBE) parameterization of the exchange correlation function.[20] We use the Heyd Scuseria Ernzerhof(HSE06) hybrid exchange-correlation

[1]Corresponding author: biaohuaw@163.com

functional to correct the band gap.[21] All energy band calculations in this paper include spin-orbit coupling to consider the influence of Te atom on the band gap. The kinetic energy cutoff is set to 1000 eV and the vacuum space is larger than 20Å. The structural optimizations are stopped until the maximum atomic force and total energy tolerance lower than 1×10^{-2} eV/Å and 5×10^{-7} eV/atom, respectively. We use the linear response method to calculate the phonon dispersion curve of 1D Te_2I single-atomic chain. [22]

3 Results and discussion

3.1 Structure and stability

We optimize the geometry of the bulk Te_2I as shown in Figure 1a. The lattice constants at the lowest energy are a = 15.91 Å, b = 4.14 Å, and c = 14.10 Å, which are consistent with the experimental results (a = 15.30 Å, b = 4.12 Å, and c = 13.69 Å).[23] In a bulk Te_2I primitive cell, each Te atom binds to the neighboring Te and I atoms to form a triangular structure stacked together in a cluster. As shown in Figure 1b, it is a direct band gap semiconductor with a band gap of 0.31 eV.

Next, We evaluate the feasibility of exfoliating 1D Te_2I single-atomic chains from bulk system by calculating the exfoliation energy E_{exf}. The calculation formula of exfoliation energy is

$$E_{exf} = \frac{E_{bulk}}{N_{bulk}} - \frac{E_{1D}}{N_{1D}} \quad (1)$$

Where $E_{bulk}(E_{1D})$ and $N_{bulk}(N_{1D})$ represent the total energy and the number of atoms in the bulk-Te_2I (1D-Te_2I) in their primitive cells, respectively. The result is 137.95 meV/atom, which is notably lower than that of 1D Te chains (~270 meV/atom), indicating that 1D Te_2I single-atomic chain structure can in principle be exfoliated from its bulk structure.[24]

(a)

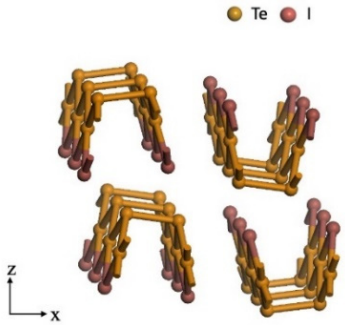

(b)

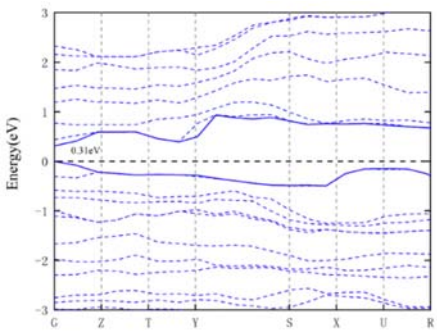

(c)

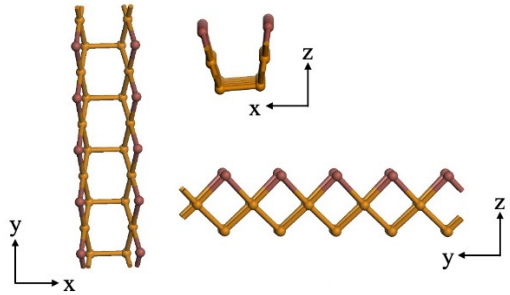

Figure 1. (a)Atomic structures of Te_2I bulk. (b)Band structure of Te_2I bulk. (c)Atomic structure of an isolated Te_2I atomic chain.

Figure 1c shows the exfoliated 1D Te_2I single atomic chain structure, and the optimized lattice constant is b = 4.12 Å(Table 1). The atomic arrangement of the single chain in the primitive cell is the same as that of the bulk system, linearly forming a chain along the b direction.

In order to check the stability of the Te_2I single-atomic chain, we first calculate its binding energy. The binding energy E_b defined as

$$E_b = \frac{mE_{Te}+nE_I-E_{total}}{m+n} \quad (2)$$

where $E_{Te}(E_I), E_{total}$, and m (n) are the total energies of an isolated Te (I) atom, a primitive Te_2I cell, and the number of Te (I) atoms in the primitive cell, respectively. The calculated E_b is 2.81 eV/atom, which is larger than that of the 1D atomic Te chains (2.51eV/atom), indicating that the Te-Te and Te-I bonds of Te_2I single-atomic chain crystal are robust.[25]

Table 1.Optimized lattice constants, exfoliation energy(E_{exf}), and binding energy(E_b) of bulk and 1D single-atomic Te_2I.

	a(Å)	b(Å)	c(Å)	$E_{exf}(meV)$	$E_b(eV/atom)$
bulk Te_2I	15.91	4.14	14.10	-	-
1D Te_2I	-	4.12	-	137.95	2.81

We then explore the kinetic stability of Te_2I single-atomic chain by computing the vibrational phonon spectrum. The phonon dispersion curves show its dynamical stability due to the absence of apparent imaginary frequency phonon modes in the entire Brillouin zone(Figure 2a).

Furthermore, We perform the *ab initio* molecular dynamics(AIMD) simulations to evaluate the thermal stability for 1D Te_2I. At temperature 300 K, we set the time step 1 fs and total simulation time 10 ps in a 1*6*1 supercell. As shown in Figure 2b, a snapshot sharp at the end of the simulation, suggesting the structural integrity maintained well.

(a)

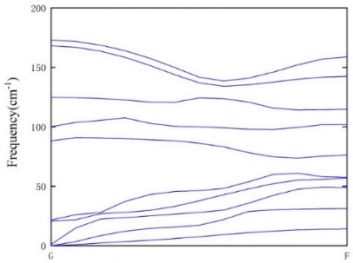

(b)

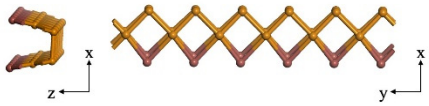

Figure 2. (a) Phonon dispersion of 1D single-atomic Te_2I. (b) Snapshots for the final configurations.

3.2 Mechanical properties

We calculate its elastic modulus to confirm the mechanical stability. The term C_{1D} defined by

$$C_{1D} = (1/L)(\partial^2 E/\partial\varepsilon^2) \quad (3)$$

L is the lattice constant along the chain direction, E is the total energy of 1D single-atomic chain structure. The value of C_{1D} along the a direction is 15.22×10^{-9} N, which is higher than that of 1D SbSBr(12.59×10^{-9}N) and 1D SbSBr(13.54×10^{-9}N), indicating 1D Te_2I crystal has the potential to be used in flexible nanoelectronic devices.[26]

3.3 Electronic structure

After confirming the structural stability of a 1D Te_2I single-atomic chain, we next investigate its electronic structure nature. As shown in Figure 3a, we give the energy band dispersion curves on the theoretical levels of PBE+SOC(HSE06+SOC), suggesting that it is an indirect band gap semiconductor with a bandgap of 1.06 (1.51) eV. The conduction band minimum(CBM) of single-atomic chain lies in the G point, whereas the valence band maximum(VBM) locates on the G-F path. The partial density of states(PDOS) shows in Figure 3b, which reveals that the VBM state is mainly formed by the hybridization of Te-5s5p and I-5p orbitals, and the Te-5p orbitals dominate the electronic states near CBM with a small amount of I-5p states.

(a)

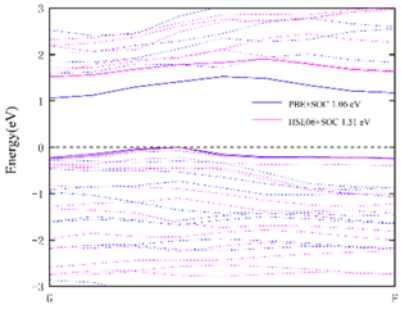

(b)

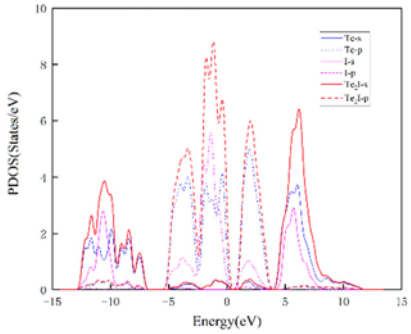

Figure 3. (a)Band structures of 1D single atomic Te_2I calculated by PBE+SOC and HSE06+SOC methods. (b)The projected density of states (PDOS) at the HSE06+SOC level.

3.4 Carrier mobilities

We estimate the carrier mobility of 1D Te_2I single-atomic chain crystal to explore its conductivity. The carrier mobility μ_{1D} is given by the formula

$$\mu_{1D} = \frac{e\hbar^2 C_{1D}}{(2\pi k_B T)^{1/2}|m^*|^{3/2}|E_1|^2} \quad (4)$$

Where $e, \hbar, k_B, T, C_{1D}, m^*$ and E_1 are electron charge, reduced Planck constant, Boltzmann constant, temperature, stretching modulus, effective mass and deformation potential constant, respectively. The calculation results of the above parameters are shown in Table 2. Therefore, at temperature 300K, the electron and hole mobilities along the chain direction are 38.43 cm^2Vs^{-1} and 7.92 cm^2Vs^{-1}, which indicates good conductivity with other 1D materials such as SbSeI($\mu_e = 25.69\ cm^2Vs^{-1}, \mu_h = 6.84\ cm^2Vs^{-1}$) and SbSBr($\mu_e = 96.68\ cm^2Vs^{-1}, \mu_h = 0.64\ cm^2Vs^{-1}$), suggesting its potential applications in microelectronics.[26]

Table 2.Calculated deformation potential constant (E_1), 1D elastic modulus (C_1D), effective mass (m^*) and mobility (μ) for electron (e) and hole (h) along b direction at 300 K.

Direction	Carrier type	$E_1(eV)$	$C_{1D}(N)$	m^*/m_0	$\mu(cm^2V^{-1}S^{-1})$
b	*e*	0.77	15.22	2.23	38.43
	h	1.31		3.14	7.92

3.5 Optical properties

To assess the light-harvesting efficiency, we calculate the absorption coefficient of a 1D Te_2I single-atomic chain crystal, as shown in Figure 4. It can be seen from the figure that the significant peak of the crystal absorption coefficient appears at ~ 136nm, and the maximum value is up to 31000 cm^{-1}, indicating that the absorption intensity of ultraviolet radiation is stronger in the ultraviolet region. In addition, its absorption coefficient maintains a high value in the range of 100-200 nm, suggesting its strong capture ability in the ultraviolet region, leading it a potential application prospect in optoelectronic devices.

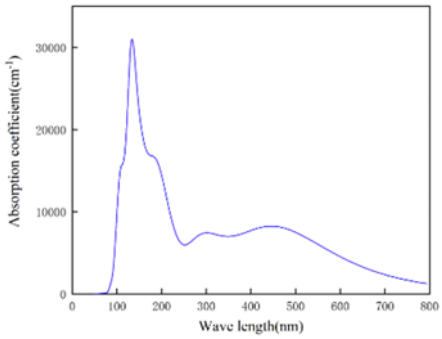

Figure 4. Calculated absorption coefficients of 1D single-atomic Te_2I at the HSE06+SOC level.

4 Conclusion

In summary, we predict a new 1D Te_2I atomic chains material based on first principles, which is an indirect band gap semiconductor with a band gap of 1.51 eV. Good electron mobility indicates that it is a candidate material for nanoelectronic devices. The exfoliation energy of 1D Te_2I single-atomic chain is 137.95 meV/atom, much lower than that of 1D Te chains, suggesting that the exfoliation from the bulk Te_2I system is feasible. The stability of kinetics and thermodynamics shows that the exfoliated 1D Te_2I structure is stable. In addition, we also studied its mechanical properties, which indicates that it has potential applications in flexible electronic devices. Finally, its absorption spectrum shows that it has a stronger light-harvesting ability in the ultraviolet region, indicating its application prospects in the field of optoelectronics.

References

1. A. Zhang, G. Zheng, and C.M. Lieber, Nanoscience and Technology **pp**, 307–310(2016).
2. A. Jorio, G. Dresselhaus, M.S. Dresseldhaus, Carbon nanotubes. Springer **11**, 57(2008).
3. S.J. Tans, A.R.M. Verschueren, C. Dekker, Nature **393**, 49–52(1998).
4. Y. Cui, X. Duan, J. Hu, C.M. Lieber, J. Phys. Chem. B **104**, 5213–5216(2000).
5. Y. Cui, Q. Wei, H. Park, C.M. Lieber, Science **293**,1289(2001).
6. W. Liang, M. Bockrath, D. Bozovic, J.H. Hafner, M. Tinkham, H. Park, Nature **411**, 665–669(2001).
7. G. Refael, J. Heo, M. Bockrath, Phys Rev Lett **98**, 246803(2007).
8. Y.J. Zhu, W.W. Wang, R. J. Qi, X. L. Hu, Angew. Chem **116**,1434(2004).
9. H. Yu, P.C. Gibbons, W.E. Buhro, J. Mater. Chem **14**, 595(2004).
10. Q. Lu, F. Gao, S. Komarneni, Adv. Mater **16**, 1629(2004).
11. J. Li, X. Tang, L. Song, Y. Zhu, Y. Qian, J. Cryst. Growth **311**, 4467-4472(2009).
12. W.I. Park, H.S. Kim, S.Y. Jang, J. Park, S.Y. Bae, M. Jung, H. Lee, J. Kim, J. Mater. Chem, 18, 875–880(2008).
13. S. Neretina, R.A. Hughes, J.F. Britten, N.V. Sochinskii, J.S. Preston, P. Mascher, Nanotechnology **18**, 275301(2007).
14. Y. Du, G. Qiu, Y. Wang, M. Si, X. Xu, W. Wu and P. D. Ye, Nano Lett **17**, 3965–3973(2017).
15. K. Kobayashi and H. Yasuda, Chem. Phys. Lett **634**, 60–65(2015).
16. H. O. H. Churchill, G. J. Salamo, S. Q. Yu, T. Hironaka, X. Hu, J. Stacy, I. Shih, Nanoscale Res Lett **12**, 488(2017).
17. E. Anastassakis, J. S. Raptis, W. Richter, Phys. Stat. Sol. (b) **130**, 161-168(1985).
18. J. D. Joannopoulos, M. Schlüter and M. L. Cohen, Phys. Rev. B **11**, 2186(1975).
19. M. D. Segall, P. J. D. Lindan, M. J. Probert, C. J. Pickard, P. J. Hasnip, S. J. Clark, M. C. Payne, J. Phys.: Condens. Matter **14**, 2717–2744(2002).
20. J. P. Perdew, K. Burke and M. Ernzerhof, Phys. Rev. Lett **77**, 3865–3868(1996).
21. J. Heyd, G.E. Scuseria, M. Ernzerhof, J. Chem. Phys **118**, 8207–8215(2003).
22. S. Savrasov and D. Savrasov, Phys. Rev. B: Condens. Matter Mater. Phys **54**, 16487–16501(1996).
23. R. Kniep, D. Mootz and A. Rabenau, Z. Anorg. Allg. Chem **422**, 17-38(1976).
24.B. Tuttle, S. Alhassan, S. Pantelides, Nanomaterials **7**, 115(2017).
25. J. Han, A. Zhang, M. Chen, W. Gao and Q. Jiang, Nanoscale **12**, 10277-10283(2020).
26. B. Peng, K. Xu, H. Zhang, Z. Ning, H. Shao, G. Ni, J. Li, Y. Zhu, H. Zhu, C.M. Soukoulis, Adv.Theor.Simul **1**, 1700005(2018).